ISSN 0001-4338, Izvestiya, Atmospheric and Oceanic Physics, 2009, Vol. 45, No. 5, pp. 598–607. © Pleiades Publishing, Ltd., 2009.
Original Russian Text © V.G. Bondur, Yu.V. Grebenyuk, K.D. Sabynin, 2009, published in Izvestiya AN. Fizika Atmosfery i Okeana, 2009, Vol. 45, No. 5, pp. 641–651.

The Spectral Characteristics and Kinematics of Short-Period Internal Waves on the Hawaiian Shelf

V. G. Bondur[a], Yu. V. Grebenyuk[a], and K. D. Sabynin[b]

[a] *Aerokosmos Scientific Center of Aerospace Monitoring, Gorokhovskii per. 4, Moscow, 105064 Russia*
e-mail: vgbondur@online.ru

[b] *Institute for Space Research, Russian Academy of Sciences, ul. Profsoyuznaya 84/32, Moscow, 117810 Russia*
e-mail: ksabinin@yandex.ru

Received November 11, 2008; in final form, March 16, 2009

Abstract—Based on the results of analyzing the characteristics of currents and temperature measured in the water space of the Mamala Bay (the Island of Oahu, Hawaii), we investigate the main properties of the field of short-period internal waves, which is very complex. We focus on analyzing the spectral characteristics and orbit parameters for waves with a period of 20 minutes. The results of investigations reveal two types of short-period internal waves for this area: intense and fast waves propagating predominantly toward the ocean and weaker and slower waves propagating mainly toward the coast. Suppositions are made on how these waves form: the strong and fast waves are likely to be caused by the decay of locally generated internal tides near the shelf edge, while the weak and slow and very short waves seem to result from the specific interaction between the pycnocline and strong tidal currents over a steep slope.

DOI: 10.1134/S0001433809050077

1. INTRODUCTION

An analysis of the radar and optical space imagery of the ocean surface near the Hawaiian Islands shows that, without special spectral processing [1–3, 13], short-period internal waves (SPIWs) cannot be revealed in this area because they occur near the edge of continental shelves [1, 4, 12, 13, 17, 18]. This may be related not only with the relatively large thickness of the upper mixing layer, but also with some specific features of the generation, propagation, and form of SPIWs near the islands. Having sufficiently detailed measurement data on the fluctuations of currents, temperature, and sound-scattering layers near the shelf edge in the Mamala Bay (the Island of Oahu, Hawaii), we tried to characterize the main features of the field of short-period internal waves (waves with periods of less than an hour).

2. A BRIEF DESCRIPTION OF BACKGROUND CONDITIONS AND ANALYZED DATA

To investigate the characteristics of internal waves on the shelf near the Island of Oahu in the water space of the Mamala Bay, we used the hydrophysical measurement data obtained in a 2004 international project [1, 2, 6, 13, 14, 19]. The hydrophysical parameters were measured with the help of a number of stationary stations equipped with thermal strings and acoustic Doppler profilers (ADPs), as well as shipboard CTD and XBT sensors and microstructure sensors (MSSs). Figure 1 shows the position of stationary stations that were fixed on the shelf edge and measured the vertical profiles of temperature (stations AT, BT, CT, and DT) and the three components of the current-field vector (stations AV, BV, and CV) for 2–3 weeks. The thermistor chains and ADPs were arranged alongside them.

The temperature and current measurements were conducted at three sites in Malama Bay (see Fig. 1):

(i) at stations AT and DT, located near a diffuser of the escape discharge system;

(ii) at stations BT and BV, 3.5 km east of the diffuser;

(iii) at stations CT and CV, ~7 km south-east of the diffuser.

At stationary stations, the currents were measured in the depth range from 4 to 76 km with a vertical step of 2 m and a time step of 1 min.

The measurements of water temperature in 2004 were conducted at different levels from 17–33 to 70–172 m with a vertical step of 5–10 m and a time step of 40 s [6, 13, 14, 19]. The data collected in view of the resolution and duration of measurements make it possible to investigate the variability of hydrophysical characteristics in the Mamala Bay in scales between several minutes and 20 days.

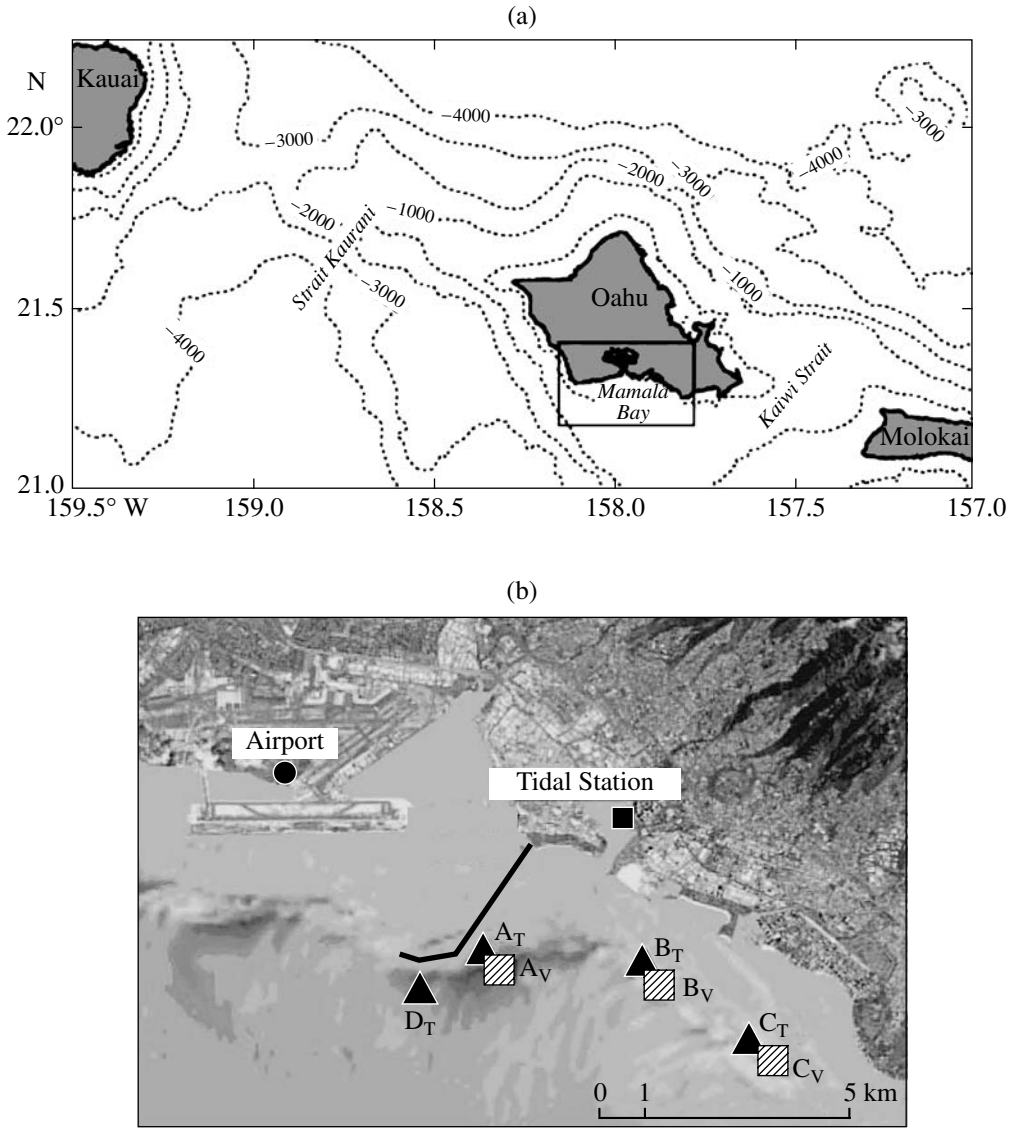

Fig. 1. (a) Geographic and bathymetric map of the water area of the Island of Oahu; (b) the distribution of stationary stations for measuring temperature and current velocity in Mamala Bay.

An analysis of the hydrophysical measurements in the Mamala Bay shows that the records of currents, temperature, and sound-scattering layers reveal (on the background of powerful multi-hour (mainly, 12- and 6-hour) oscillations) episodic wavetrains and solitary short-period internal waves with more or less significant amplitudes [4–6]. Unlike the waves observed in other areas [1, 12, 23], these are not quasi-sinusoidal waves, and they appear as solitary waves and wavetrains with a small number of oscillations. In addition, these internal waves are highly inferior to low-frequency waves in amplitude, as can be easily seen in Fig. 2. This figure shows the oscillations of isotherms in the range between 23.5 and 28°C under the action of internal waves, registered at the station AT on September 3, 2004.

It can be seen from Fig. 2 that the isotherm oscillations are of a complex character: apart from the dominating semidiurnal waves, there are 6-hour waves of almost the same power and the soliton-like oscillations appear as both depression and elevation solitons. It should be noted that the solitons are observed not only in the low-frequency wave troughs (as normally occurs [12]), but also near their crests. For example, it can be seen from Fig. 2 that, at the 6–9-h period, the 4-hour wave crest is characterized by a passing wavetrain of several depression solitons, while there is wavetrain of elevation solitons at the back slope of the next wave at 13–15 h.

This unusual character of solitons in the area and the relatively weak manifestation of their wavetrains are connected with fact that the pycnocline axis is

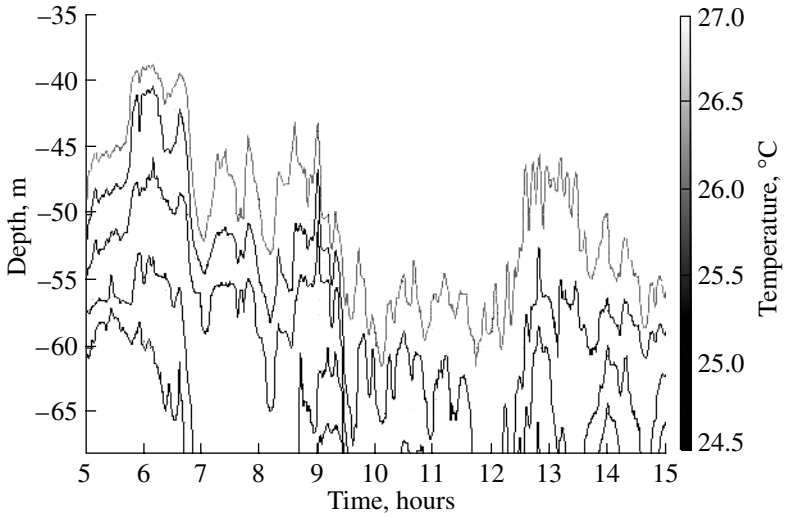

Fig. 2. Oscillations of isotherms under the action of internal waves registered at station AT on September 3, 2004.

located near the middle of the water column. In these conditions, the generation of solitons is hampered; at significant oscillations of the pycnocline depth, solitons of either polarity may be generated (depression solitons are dominant for a high pycnocline, and elevation solitons are dominant for a low pycnocline). Figure 3 illustrates the strong oscillations of the pycnocline depth in the area of the Oahu Island.

In view of the complex character of SPIWs in the area under consideration, our main focus was on the average characteristics of the field of these waves by analyzing the isotherm and current oscillation spectra.

3. AN ANALYSIS OF HYDROPHYSICAL MEASUREMENT DATA IN MAMALA BAY

To study the parameters of short-period internal waves in Mamala Bay, we use contact measurement data to calculate and analyze the spectral characteristics of fluctuations of current velocities and isotherms, orbit parameters of horizontal currents, variations in the amplitude of SPIWs and their coherence with internal tides, and phase velocities and the divergence of orbital currents of SPIWs. Let us consider the main results of these studies.

Figure 4 shows the spectra of vertical velocities of the thermocline shifts estimated by oscillations of the occurrence depths of the central isotherm of the thermocline (27°C) at stations BT and CT in 2004. The spectra were calculated for the frequency range 0.02–60 c/h and are represented in the semi-logarithmic scale. The fluctuations of vertical velocities in the frequency area above 20 c/h were smoothed using a fourth-order Butterworth filter. It can be seen from Fig. 4 that the spectra include a wider peak at frequencies 3–5 c/h, along with the narrow semidiurnal and 5–6-h peaks.

At the same time, no short-period internal waves can be found at the frequency spectra of currents shown in Fig. 5. This can be explained by the general tendency for the role of horizontal motions to decrease with the frequency growth in a random field of internal waves [15].

3.1. Analysis of Current Characteristics

An analysis of the current-field characteristics measured with the help of the ADP reveals an increased level of noise interference. To reduce the measurement errors, we averaged the initial data by depth and time. The results of investigations show that smoothing by depth is especially efficient. The most optimal method of smoothing by depth is the fourth-order Butterworth filter with a cut frequency of 100 c/km when the signal–noise ratio exceeds 1 at frequencies below 4 c/h. At higher frequencies, the noise prevails, which limits the frequency band in studying SPIWs by ADP data.

When processing ADP data, we also take into account the signal attenuation and ray divergence as the distance from the instrument grows. Near the boundaries of the measurement-covered layer, the emerging terminal effects of the smoothing filter by depth are observed. In view of this, we restrict ourselves to an analysis of the current-velocity data for the 10–70-m layer.

Particular emphasis has been placed on the measurement errors for the vertical velocity W, which appear due to errors in determining the slope of ADP rays. Because of this, the results of measurements of W may be distorted through the "leakage" of the horizontal components of the current, even if the resolution of ray-slope measurements is 1°. Such "pollution" is particularly essential at low frequencies,

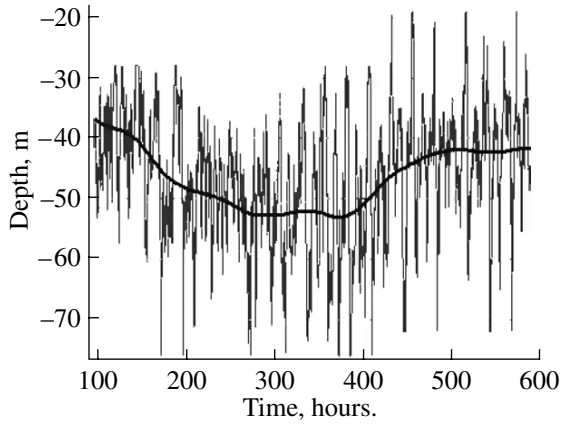

Fig. 3. Oscillations of the depth of isotherm 27°C (the central isotherm of the pycnocline) and its smoothed value by measurements at station BT.

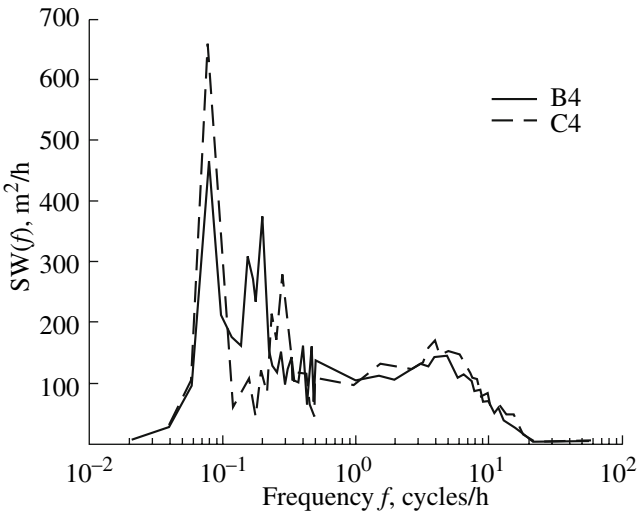

Fig. 4. Spectra of vertical velocities of shifts in the thermocline occurrence depth *Sw*(*f*) estimated by oscillations of the isotherm 27°C at stations BT and CT in 2004.

where the vertical velocities are lower than the horizontal layers.

Figure 5 presents the spectra of horizontal currents and average orbit parameters of SPIWs calculated by the method of spectral invariants of currents [9].

It should be noted that, in the plots shown in Fig. 5, the direction of orbit axes is given in the mathematical system of degree indications (from the counterclockwise eastern direction).

It can be seen from Fig. 5 that the spectra of horizontal currents fall in frequency uniformly and without peaks, but their average orbits in the frequency range 2–4 c/h are relatively stable and narrow. The orbits have a southwestern direction; i.e., they are directed across the isobaths that deviate from the par-

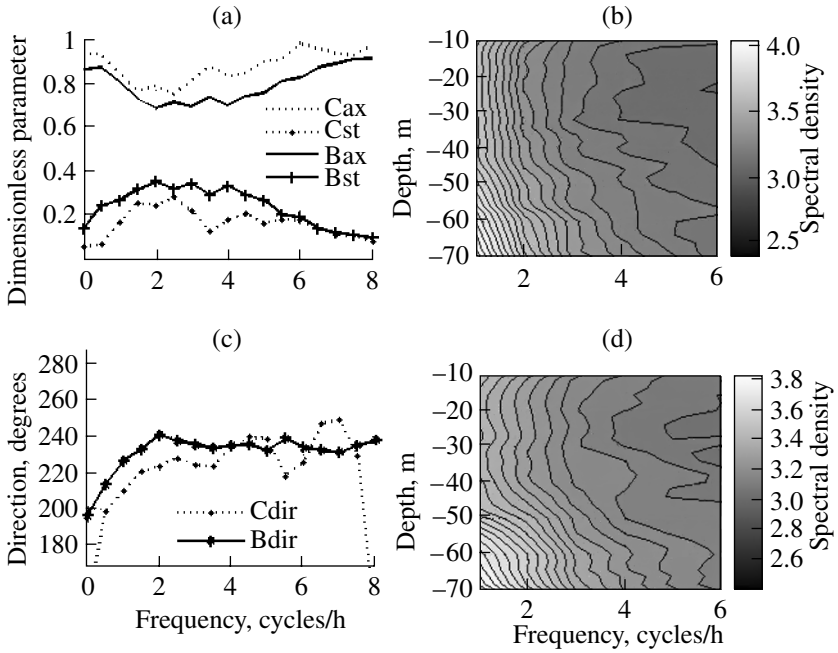

Fig. 5. (a, c) Orbit parameters of horizontal currents calculated by measurement data at a depth of 70 m at stations B and C; ratio of minor and major orbit axes (ax), their stability rate (st); (b, d) direction of the major axis (dir), and spectra of meridian currents in the frequency–depth coordinate system at stations C (b) and B (d).

allel by 37° near the station B and by 52° near the station C.

As known from [7, 8], in the case of unidirectional internal waves, their orbital currents are alternating. The measured parameters of orbits of horizontal currents (namely, the nonzero ratio of orbit axes and the deviance of their stability from unity) point to the rather complex spatial and temporal structure of the field of SPIWs in this area. Nevertheless, the fact that the observed average orbits near the frequency 3 c/h are slightly elongated and stable, as well as the corresponding SPIWs expressed on the spectra of vertical oscillations of the thermocline (see Fig. 2), allow us to separate 20-min waves out of the general background of rather chaotic oscillations. Hereafter, we will consider these waves in particular.

At both points, the variability of 20-min-wave parameters (intensity, rate of directivity, and wave direction) was very significant with the clearly expressed dominance of the semidiurnal period. To study the intensity oscillations of 20-min waves, we used sliding values of rms amplitudes in the frequency band of around 3 c/h, which were calculated in 2-hour intervals overlapped by 1 hour. To estimate the relation of this intensity with the low-frequency oscillations of the thermocline, we calculated the corresponding coherence on the example of oscillations of the depth of the 27° isotherm (central isotherm of the thermocline) at the point B4 (see Fig. 6b).

It can be seen from Fig. 6 that the maximum level of coherence was at the semidiurnal period. The difference between the thermocline oscillations and the intensity of 20-min waves was 141°; i.e., the most intensive SPIWs were near the trough of the internal tide (IT) rather than at the crest. If similar waves were also near the IT crests, the main peak of coherence would be at the 6-hour period because the rms (i.e., always positive) amplitude of SPIWs was used.

The semidiurnal and quarter-diurnal peaks on the amplitude variation spectra of 20-min waves (see Fig. 6a), as well as the bursts of coherence of this variability with low-frequency motions at semidiurnal and quarter-diurnal periods (see Fig. 6b), point to the relation of these waves with ITs. The absence of coherence between the isotherm oscillations and intensity of 20-min along-shore currents, as well as the noticeable relation with the intensity of currents across the isobaths (see Fig. 6b), is consistent with the earlier established directivity of waves (see Fig. 5). All these characteristics point to the relation of SPIWs with ITs generated locally near the shelf edge rather than with the waves coming from afar and propagating along the isobaths, although it is these waves that dominate in the field of ITs in Mamala Bay [11, 17, 20, 21].

The coherence of currents of different directions with the thermocline oscillations also takes maximum values if the direction is across the isobaths (Fig. 6c). It should be noted that the coherence peak at a frequency of 3.5 c/h and for a direction of 240° corresponds to an almost vanishing difference of phases 13° (Fig. 6d), as should be expected for the low-mode waves traveling to the shore where the oscillations of the pycnocline depth and orbital currents in the lower layer are co-phased.

Using the processing method developed, which makes it possible to estimate the phase velocity of narrow-directed waves by ADP data [20], we calculated the parameters of 20-min waves directed across the isobaths. This method uses a continuity equation and data on the horizontal U and V and vertical W components of currents at three levels in the layer where the waves are well expressed both in horizontal velocity and the vertical gradient of vertical velocity dW/dz.

The essence of the method is in the following. If a wave travels along the 0y-axis, the continuity equation has the form

$$V_y + W_z = 0, \quad (1)$$

where V_y and W_z are the partial derivatives with respect to the 0y and 0z axes, respectively.

For a sinusoidal wave, we have

$$V = \sin(Ft - Ky), \quad (2)$$

where F is the circular frequency and K is the wave number in the meridian direction:

$$V_t = F\cos(Ft - Ky) \quad \text{and} \quad V_y = -K\cos(Ft - Ky), \quad (3)$$

where V_t is the partial derivative with respect to time.

Because the phase velocity of the wave $C = F/K$, we have

$$V_y = -V_t/C, \quad (4)$$

which, in view of the continuity equation, yields

$$C = V_t/W_z. \quad (5)$$

The phase velocities of SPIWs were analyzed for the waves observed in the layer between 58 and 70 m. We consider the cases when the across-isobath V components of currents exceed the along-shore velocity U (the condition of narrow directivity) by more than 10 times, while the gradient W_z and V had large enough values to disregard the possible measurement errors. The influence of wave transfer by the average current was eliminated by extracting the depth-averaged current so that the wave velocity was estimated relative to the water.

The results of calculations of the phase velocity Cp for station B4 are presented in Fig. 7 as one-dimensional (Fig. 7a) and three-dimensional (Figs. 7b and 7c) histograms. Here, the direction to the shore corresponds to positive velocities and the direction from the shore corresponds to negative velocities. An analysis of the data presented in Fig. 7 shows that waves that propagate to the shore are clearly dominant. In this case, waves with phase velocities Cp ~ 0.2 m/s,

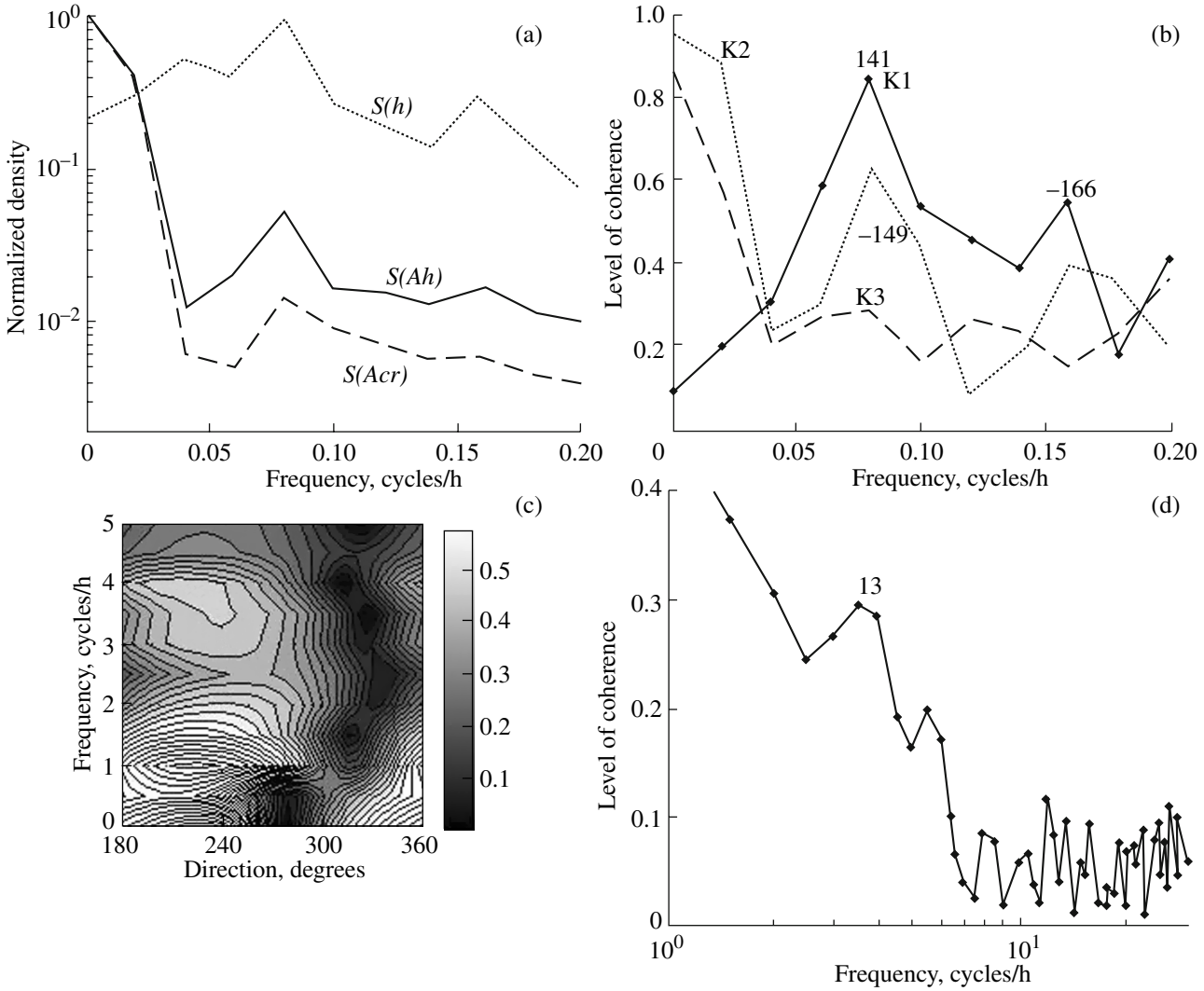

Fig. 6. Relation of (a, b) variations of the amplitude of 20-min waves with low-frequency motions, (c, d) high-frequency oscillations of the thermocline and currents at station B4; (a) normalized spectra $S(h)$ of oscillations of the isotherm depth, amplitude $S(Ah)$ of 20-min oscillations of the isotherm, and amplitude $S(Acr)$ of 20-min currents directed across the isobaths; (b) plots of coherence K: oscillations of the isotherm and amplitude of 20-min waves (K1), baroclinic currents at a depth of 70 m along an across the isobaths with amplitude variations of corresponding 20-min waves ((K2) transverse waves and (K3) longitudinal waves, with numbers near the coherence peaks showing the phase difference of oscillations); (c) coherence of minutely baroclinic currents of different directions at a depth of 70 m with minute oscillations of depth of the isotherm 27°; (d) coherence of minutely baroclinic currents across the isobaths at a depth of 70 m with minute oscillations of depth of the isotherm 27°.

where the vertical velocities W were small (lower than 0.1 cm/s), were the most repeated; the positive and negative divergences occurred with similar frequencies. The slight divergence $|\mathrm{div}V| < 0.0003$ s^{-1} was disregarded because it does not go beyond the limits of estimation error.

The faster (Cp ~ 0.5 m/s) and more intensive (W ~ 0.5 m/s) internal waves traveling to the ocean with the velocity of the lowest mode (the peak in the lower-right quadrant in Fig. 7b and the "relief" ridge in Fig. 7c) were somewhat rare.

Similar histograms were also constructed for station C4, where the duration of velocity measurements was shorter and the number of estimates for phase velocities obtained was smaller. Like at the point B4, weak and slow (Cp = 0.2 m/s) internal waves traveling to the shore were more frequent. The faster (Cp = 0.5 m/s) and more intense internal waves traveled to the ocean.

The faster and more intense (but rarely occurring) wave components of the field of SPIWs seem to be related to episodic soliton-like wavetrains, which are not clearly expressed but can be found in the area under consideration.

Now, let us consider the vertical structure of SPIWs by using dynamical (calculated on the basis of buoyancy frequency observed in the area) and empir-

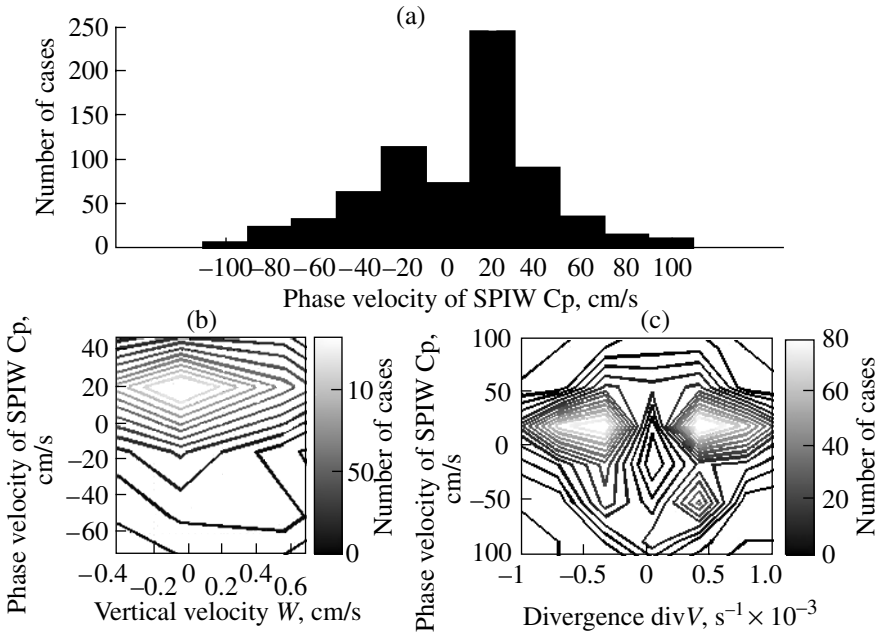

Fig. 7. Histograms of phase velocities of SPIWs using measurements at station B4 of (a) the periodicity of the phase velocity of 20-min transverse waves directed to the shore (Cp > 0) and from the shore (Cp < 0) and (b) a three-dimensional histogram of horizontal divergence div$V$ and Cp.

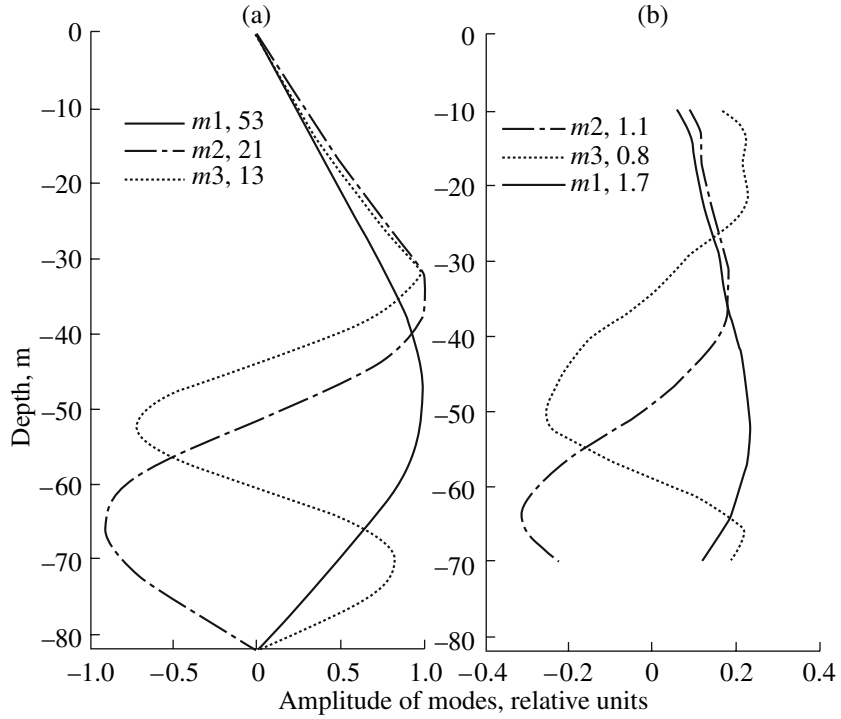

Fig. 8. Normalized profiles of the vertical-velocity amplitude for the modes 1–3 of 20-min waves: (a) dynamical modes (calculated by the buoyancy frequency N) and (b) empirical modes. The numbers in the legends indicate (a) the phase velocities and (b) the rms amplitudes of modes in cm/s.

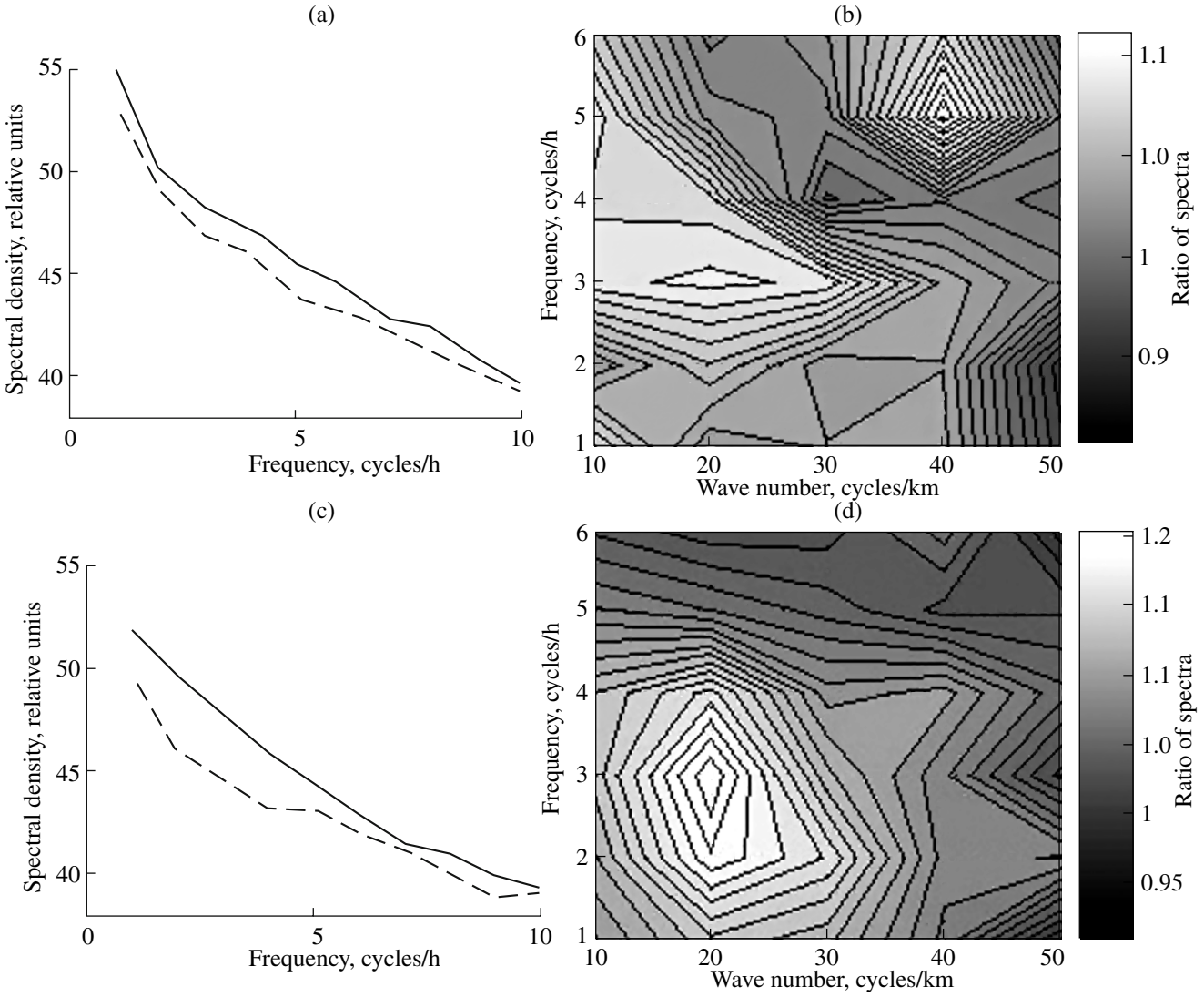

Fig. 9. Asymmetry of SPIW energy fluxes at stations (a, b) C4 and (c, d) B4. (a, c) Frequency spectra of the vertical velocity in waves going (by energy) upward (solid line) and downward (dashed line); (b, d) ratio of spectra of upward and downward going waves.

ical eigenfunctions of vertical velocities in 20-min internal waves (Fig. 8).

The profiles of dynamical and empirical modes are similar to one another; however, the difference between them grows as the mode number increases. This indicates that the amplitude of empirical modes decreases rather weakly with the mode number, which reduces the quality of wave-field approximation with the help of modes. We could conclude that the number of field-forming modes was significantly higher, but the following fact prevents us from doing so. The SPIWs propagate in the pycnocline, whose depth in the area under consideration is highly variable (by 30–50 m) under the influence of powerful ITs and other low-frequency processes (see Fig. 2 and [4, 5]). In this case, the nodes and antinodes of eigenfunctions follow the "rocking" waveguide, which leads to "smearing" of the average pattern and to apparent multimode oscillations even if the vertical structure of oscillations is simple.

The tidal currents that are dominant in the area distort both the profiles of modes of internal waves and dispersion relations. However, for average characteristics of internal waves, the influence of variable currents can be disregarded, because they merely "smear" the modes and lead to no cardinal changes in the average dispersion characteristics.

In addition, there are not only vertically standing modes near the source of internal waves, and this is observed in our case. Indeed, the spectra of vertical velocities calculated separately for the waves with ris-

ing and dropping energy (Fig. 9) reveal that the rising waves in the frequency band 1–10 c/h are dominant. The asymmetry is particularly noticeable at a frequency of 3 c/h for a vertical wavelength of 50 m. At the station C4, the asymmetry is somewhat weaker than at B4. In this case, the asymmetry is expressed not only at 3 c/h, but also at 5 c/h for a wavelength of 25 m.

This asymmetry points to the bottom generation of the corresponding waves forming a quasi-mode structure only after the reflection in surface layers.

4. DISCUSSION OF RESULTS

On the basis of a comprehensive spectral analysis and using new methods of data processing, we managed to reveal the main properties of SPIWs in the water area of Mamala Bay, which is characterized by great complexity without a clear dominance of spectral components. Fifteen-to-twenty-minute internal waves are not definitely expressed as a wide peak on the spectrum of isotherm-depth oscillations, unlike the spectra of currents smoothly falling with frequency. These 15–20-min oscillations appear in such characteristics of current spectra as stability and directivity of ellipses of orbital motions. For the corresponding oscillation frequencies, there is an observed rise in both the stability and directivity of ellipses of orbital motions. This makes it possible to separate 15–20-min internal waves out of the general background of oscillations with a continuous spectrum. Characteristics of these waves such as the directivity across isobaths, the large phase velocity for most energetic components, and the clear relation between wave intensity and ITs are consistent with the commonly accepted view on the local generation of SPIWs when ITs break down into soliton wavetrains near the shelf boundary [23]. At the same time, the unique feature of slow components (complex modal structure and asymmetry of vertical spectrum) indicates that they are generated quite normally. In the area under consideration, the intensive waves (possibly soliton-like wavetrains) traveled predominantly into the ocean, whereas the weaker and slower components of 20-min waves propagate mainly to the shore.

The way these small but frequently occurring waves actuate is not entirely known. Supposedly, they are also generated by tidal currents (both barotropic and baroclinic), which obtain significant vertical velocities near the very steep edge of the shelf. Indeed, the tidal current jets streamlining the steep bottom "hit" the pycnocline at a large angle, which should make it oscillate at a resonance frequency. In this case, the resonance frequency is the frequency of oblique wave F_c determined by the bottom slope (i.e., also by the slope of tidal current jets streamlining the bottom) and buoyancy frequency N near the shelf edge:

$$F_c = N\sin A, \tag{6}$$

where A is the angle of bottom slope (close to 30°). Taking N = 9 c/h (a vertically averaged value near the shelf edge), we obtain

$$F_c = 9\sin 30° = 4.5 \text{ c/h}, \tag{7}$$

which is close to the frequency of SPIWs dominating in the area.

This hypothesis of the origination of 15–20-min oscillations in the area under consideration explains their other properties too; namely, the asymmetry of the vertical spectrum and clear presence of higher modes, appearing in their small velocities and complex vertical structure. In other words, the oscillations generated by oblique jets of tidal currents should also have an oblique component described by many modes.

CONCLUSIONS

Based on the results of an analysis of the characteristics of SPIWs in the water space of the Mamala Bay, we can make the following conclusions. In the complex field of these internal waves, there are relatively narrow-directed 15–20-min oscillations of two types: (1) frequently occurring weak and slow waves traveling to the shore and (2) faster and more intense waves traveling to the ocean.

Apparently, the slow, weak, and very short (with a length of 100–200 m) waves are actuated as a result of a specific interaction between the pycnocline and strong tidal currents over the steep slope. They propagate to the shore at a rate of 2–4-mode waves and a slight dominance of upgoing energy. The faster and stronger waves, traveling to the ocean at the rate of the lowest mode, are likely to be related with the breakdown of locally generated ITs, occurring normally near the shelf edge. The relative weakness of emerging wavetrains of soliton-like waves is explained by the shore adjacency and the fact that the density stratification of waters in the Mamala Bay is unfavorable for their generation. The pycnocline, which is subjected to strong oscillations in the bay, is located in the middle of the water layer; as a result, the solitons are actuated only at its high or low position.

The superposition of short waves of different origins (including open-ocean waves [10, 16] traveling to the shelf), along with the weakly expressed episodic solitons, gives a special character to the field SPIWs in the shelf of the Island of Oahu (this may be characteristic of other island shelves with steep slopes).

REFERENCES

1. V. G. Bondur, "Aerospace Methods in Modern Oceanology," in *New Ideas in Oceanology.* Vol. 1 (Nauka, Moscow, 2004) [in Russian].
2. V. G. Bondur and A. Sh. Zamshina, "Study of High-Frequency Internal Waves at the Boundary of the Shelf by the Spectrum of Aerospace Optical Images," Izv. Vuzov. Sek. Geodez. Aerofotos., No. 1, 85–96 (2008).
3. V. G. Bondur, Yu. V. Grebenyuk, and E. G. Morozov, "Aerospace Recording and Modeling of Short-Period Internal Waves in the Oceanic Coastal Zones," Dokl. Akad. Nauk **48** (4), 543–548 (2008).
4. V. G. Bondur, K. D. Sabinin, and Yu. V. Grebenyuk, "Variability of Internal Tides on the Shelf of Oahu Island (Hawaii)," Okeanologiya **48** (5), 661–671 (2008).
5. V. G. Bondur, Yu. V. Grebenyuk, and K. D. Sabinin, "Characteristics of Generation of Internal Tides near Oahu Island in Hawaii," Okeanologiya **49** (2), 1–11 (2009).
6. V. G. Bondur, N. N. Filatov, Yu. V. Grebenyuk, et al., "Studies of Hydrophysical Processes during Monitoring of the Anthropogenic Impact on Coastal Basins Using the Example of Mamala Bay of Oahu Island in Hawaii," Okeanologiya **47** (6), 827–846 (2007) [Oceanology **47** (6), 769–788 (2007)].
7. K. V. Konyaev, "Semidiurnal Inclined Internal Waves in the Pycnocline from the Data on the Vertical Profiles of the Arctic Current," Izv. Akad. Nauk, Fiz. Atmosfery Okeana **38** (6), 848–85 (2002) [Izv., Atmos. Ocean. Phys. **38** (6) 755–765 (2002)].
8. K. V. Konyaev and K. D. Sabinin, *Waves in the Ocean* (Gidrometeoizdat, St. Petersburg, 1992) [in Russian].
9. V. A. Rozhkov, *Methods of Probabilistic Analysis of Oceanological Processes* (Gidrometeoizdat, Leningrad, 1979) [in Russian].
10. K. D. Sabinin and V. A. Shulepov, "On the Model of Frequency Spectrum of Internal Oceanic Waves," Izv. Akad. Nauk SSSR. Fiz. Atmos. Okeana **17** (1), 67–75 (1981).
11. M. H. Alford, M. C. Gregg, and M. A. Merrifield, "Structure, Propagation and Mixing of Energetic Baroclinic Tides in Mamala Bay," J. Phys. Oceanogr. **36**, 997–1018 (2006).
12. J. R. Apel, L. A. Ostrovsky, and Y. A. Stepanyants, Internal Solitons in the Ocean, Report GOA, Nos. 98–3 (1998).
13. V. G. Bondur, "Complex Satellite Monitoring of Coastal Water Areas," in *Proc. of 31 Int. Symp. on Remote Sensing of Environment* (St. Petersburg, 2005).
14. V. G. Bondur and N. N. Filatov, "Study of Physical Processes in Coastal Zone for Detecting Anthropogenic Impact by Means of Remote Sensing," in *Proc. of the 7 Workshop on Physical Processes in Natural Waters* (Russia, Petrozavodsk, 2003), pp. 98–103.
15. N. P. Fofonoff, "Spectral Characteristics of Internal Waves in the Ocean," Deep-Sea Res. **16**, 58–71 (1969).
16. C. Garrett and W. Munk, "Space–Time Scales of Internal Waves: A Progress Report," J. Geophys. Res. **80**, 291–297 (1975).
17. P. E. Holloway and M. A. Merrifield, "On the Spring-Neap Variability and Age of the Internal Tide at the Hawaiian Ridge," J. Geophys. Res. **108** (C4), 3126 (2003).
18. C. R. Jackson and J. R. Apel, "An Atlas of Internal Solitary-Like Waves and Their Properties," Global Ocean Associates (2002).
19. R. Keeler, V. Bondur, and C. Gibson, "Optical Satellite Imagery Detection of Internal Wave Effects from a Submerged Turbulent Outfall in the Stratified Ocean," Geophis. Res. Letters **32**, L12610, doi: 10.1029/2005GL022390/ (2005).
20. M. A. Merrifield and M. H. Alford, "Structure and Variability of Semidiurnal Internal Tides in Mamala Bay, Hawaii," J. Geophys. Res. **109**, C05010, doi: 10.1029/2003JC002049 (2004).
21. M. A. Merrifield and P. E. Holloway, "Model Estimates of M2 Internal Tide Energetics at the Hawaiian Ridge," J. Geophys. Res. **107** (C8), 3179 doi: 10.1029/2001JC000996 (2002).
22. K. Sabinin, "Divergence and Filamentation of the Sea Currents at the Shelf Edge," in *Abstracts. Int. Conf. "Fluxes and Structures in Fluids"* (St.-Petersburg, 2007), pp. 100–101.
23. K. D. Sabinin and A. N. Serebryany, Intense Short-Period Internal Waves in the Ocean, J. Marine Res. **63**, 227–261 (2005).